Frontiers in Bioscience Landmark

Front. Biosci. (Landmark Ed) **2023**; 28(5): 89
https://doi.org/10.31083/j.fbl2805089

Original Research

Upregulation of LPGAT1 Enhances Lung Adenocarcinoma Proliferation

Huiyuan Gong[1,†], Chao Ma[2,3,4,†], Xiaojun Li[1], Xueying Zhang[2,3,4], Linxiang Zhang[2,3,4], Pengfei Chen[1], Wei Wang[1], Yannan Hu[1], Ting Huang[1], Nan Wu[2,3,4,*], Xiaojing Wang[2,3,4,*]

[1]Department of Thoracic Surgery, First Affiliated Hospital, Bengbu Medical College, 233000 Bengbu, Anhui, China
[2]Anhui Province Key Laboratory of Clinical and Preclinical Research in Respiratory Disease Bengbu Medical College, 233000 Bengbu, Anhui, China
[3]Molecular Diagnosis Center, First Affiliated Hospital, Bengbu Medical College, 233000 Bengbu, Anhui, China
[4]Department of Pulmonary and Critical Care Medicine, First Affiliated Hospital, Bengbu Medical College, 233000 Bengbu, Anhui, China
*Correspondence: bbmcwunan@163.com (Nan Wu); wangxiaojing8888@163.com (Xiaojing Wang)
[†]These authors contributed equally.
Academic Editor: Elena Levantini
Submitted: 15 November 2022 Revised: 3 March 2023 Accepted: 14 March 2023 Published: 11 May 2023

Abstract

Background: Lung adenocarcinoma (LUAD) is one of the leading causes of cancer-related mortality. Lysophosphatidylglycerol acyltransferase (LPGAT1) regulates the biosynthesis of triacylglycerol, which is essential for maintaining phospholipid homeostasis and modulating the structural integrity of mitochondrial membranes. LPGAT1 has been demonstrated to be differentially expressed in normal lung tissue and LUAD tissues, and can serve as a metabolically relevant gene with potential prognostic value. However, the potential role of LPGAT1 in LUAD is still unknown. This study sought to determine the role of LPGAT1 in LUAD progression. **Methods**: LPGAT1 expression was examined in LUAD cells and tumor tissues from LUAD patients. The effect of LPGAT1 was then assessed in both cell and animal models after LPGAT1 was knocked down by RNA interference. **Results**: LPGAT1 was upregulated in LUAD tissues. Overexpression of LPGAT1 was associated with an unfavorable prognosis in LUAD patients, as revealed by univariate and multivariate Cox analyses. Knockdown of LPGAT1 abrogated tumor growth and proliferation in both cell and animal models. **Conclusions**: This study demonstrates that LPGAT1 promotes proliferation and inhibits apoptosis in LUAD. Hence, LPGAT1 may provide new treatment strategies for LUAD.

Keywords: lung adenocarcinoma; LPGAT1; phosphatidylglycerol metabolic process; lung cancer

1. Introduction

Lung cancer (LC) has become one of the most deadly malignancies worldwide [1,2]. The predominant histopathologic subtype of LC is non-small cell lung cancer (NSCLC), which accounts for over 80% of all LCs [3,4]. Lung adenocarcinoma (LUAD) is the most common subtype of NSCLC, with a 5-year survival rate of approximately 15% [5,6]. Recently, much progress has been achieved in the study of driver oncogenes, including mesenchymal lymphoma kinase and epidermal growth factor receptor [7,8]. However, resistance to targeted therapies against these genes is a significant limitation for patients. Therefore, it is of utmost importance to explore new therapeutic mechanisms for LUAD in clinical practice [9].

Lysophosphatidylglycerol acyltransferase (LPGAT1) is encoded by a gene on chromosome 1q32.2, which was originally cloned in 2004 [10]. It has been reported that LPGAT1 regulates the biosynthesis of triacylglycerol, which is essential for maintaining phospholipid homeostasis and modulating the structural integrity of mitochondrial membranes [11]. LPGAT1 has also been shown to be primarily involved in lipid metabolism, and its effects on body mass index and body fat have been confirmed [12]. These effects of LPGAT1 on the organism occur when it is in its regular expression profile. However, at levels beyond normal expression, it may lead to the development of certain diseases. Previous studies have shown that LPGAT1 gene expression is upregulated in tumor tissue compared to normal tissue, suggesting that LPGAT1 may be a potential target for the diagnosis of LUAD [13–15]. Therefore, LPGAT1 is a metabolically relevant gene with prognostic significance, and may be a new therapeutic and diagnostic target for LUAD.

In this study, by analyzing the results of the LUAD-TCGA database, LPGAT1 was found to be upregulated in LUAD tissue compared to normal tumor-adjacent lung tissue. Univariate and multivariate Cox analyses revealed that LPGAT1 was related to an unfavorable prognosis in LUAD patients. LPGAT1 expression was analyzed in LUAD cells and lung tumor tissues from patients. It was found that LPGAT1 was overexpressed in LC tissues. Subsequently, the functional roles of LPGAT1 were examined in both cell and animal models. On a cellular level, LPGAT1 promoted cell proliferation and inhibited apoptosis in LUAD. In mouse models, knockdown of LPGAT1 reduced the growth of the LUAD xenograft. The transcriptome analysis of the H1299

cell line indicated that LPGAT1 knockdown upregulated the phosphatidylglycerol metabolism pathway. However, validation of the associated mechanisms requires more extensive investigation. In summary, the findings in the present study indicate that up-regulation of LPGAT1 facilitates the oncogenesis of LUAD.

2. Materials and Methods

2.1 Tissue Collection

Between October 2018 and December 2019, 60 pairs of LUAD and neighboring lung tissues were obtained from LUAD patients in the First Affiliated Hospital of Bengbu Medical College (Anhui Province, China). All subjects underwent surgery after obtaining informed consent. This research was approved by the Ethics Committee of the same institute, and was in compliance with the standards established by the Declaration of Helsinki. After snap-freezing in liquid nitrogen, the samples were kept at –80 ℃ until further analysis.

2.2 Immunohistochemistry (IHC)

The tissue specimens were fixed in 4% formalin, embedded in paraffin, and sectioned at 4 μm thickness using a microtome. The sections were then exposed to 3% H_2O_2 to inhibit endogenous peroxidase activities, followed by heating at 95 ℃ for 20 min in 10 mM citrate buffer (pH 6.0) for antigen retrieval. To prevent non-specific binding, 0.4% triton-X100 (P0096, Beyotime, Shanghai, China) + 10% bovine serum albumin (BSA, ST023, Beyotime, Shanghai, China) was used at room temperature (RT) for 1 h. Next, these sections were cultured with LPGAT1-specific antibody (ab230647, Abcam, Waltham, MA, USA) at 37 ℃ for 60 min, followed by incubation with the secondary antibodies (PV-6000, Zsbio, Beijing, China). DAB chromogenic agent (ZLI-9018, Zsbio, Beijing, China) was then used for nucleus staining at RT for 10 min. Finally, the stained sections were examined using an microscope (CX43, Olympus, Tokyo, Japan).

2.3 Cell Culture and Transfection

Human LUAD cell lines (PC9, H1299, A549 and H23) and HEK-293T cell line were supplied by the Institute of Cell Research, Chinese Academy of Sciences (Shanghai, China). All cell lines were tested for mycoplasma and no mycoplasma contamination was observed. All cell lines were detected by short tandem repeat (STR) and all were detected correctly. All cells were cultured in DMEM containing 10% fetal bovine serum (FBS, A3160802, Gibco, Grand Island, NY, USA), and 10 mg/mL penicillin-streptomycin (PS, 15140122, Gibco, Grand Island, NY, USA). Cells were grown at 37 ℃ in an appropriate incubator with 5% CO_2.

2.4 Gene Silencing

LPGAT1 knockdown was performed by siRNA and shRNA viruses. siLPGAT1 and siCtrl were the experimental and control groups, respectively. H1299 and A549 cells were transfected with siLPGAT1 and siCtrl. The target sequences of siLPGAT1 and siCtrl are displayed in **Supplementary Table 1**. shLPGAT1 and shCtrl were cloned into pLKO.1 plasmid, followed by sequencing. The shRNA-pLKO.1 and helper plasmids (delta8.9 and VSVG) were transfected into HEK293T cells for 3 days. Lentiviruses were generated, collected, and purified via ultracentrifugation. The viral titer was determined by evaluating the infectious capacity of HEK293T cells. Stable, transfected cells were screened with 2 μg/mL puromycin (ST551, Beyotime, China). Subsequently, quantitative real-time reverse transcription PCR (qRT-PCR) and western blot (WB) analyses were conducted.

2.5 Cell Counting Kit-8 (CCK-8) Assay

The lentivirus-infected H1299 and A549 cells (1000 cells/well) were grown in a 96-well plate, followed by incubation at 37 °C. At 1, 2, 3, 4 and 5 days, 10 μL of cell counting kit -8 (CCK8, BL001B, Biomiky, Shanghai, China) was added to each well. After 4 h, the absorbance was determined using a microplate reader (F50, Tecan, Männedorf, Switzerland) at 450 nm.

2.6 Flow Cytometry (FC) Analysis

To evaluate the impact of LPGAT1 on apoptosis, the treated H1299 and A549 cells (5×10^5) were collected and stained with Annexin VFITC/PI (22837, AAT Bioquest, Sunnyvale, CA, USA). Cell apoptosis was evaluated using the FACS Calibur (FACSCanto, BD, San Jose, CA, USA).

2.7 Automated Cell Cycle Profiling and Analysis

To assess the effect of LPGAT1 on the cell cycle, A549 and H1299 cells (1×10^6) were harvested and fixed with 70% ethanol at 4 ℃ for 1 h. After rinsing twice with phosphate buffered saline (PBS, C10010500BT, Gibco, Grand Island, NY, USA), the cells were added into 2 mg/mL propidium (PI, C1052, beyotime, Shanghai, China) and 10 mg/mL RNase A (C1052 ,Beyotime, Shanghai, China), followed by incubation at 4 ℃ for 30 min in the dark. PI fluorescence intensity was measured using FACS Calibur.

2.8 Colony Formation Assays (CFA)

H1299 (or A549) cells were exposed to sh-LPGAT1 or sh-Ctrl lentivirus and cultured for 2 days. The cells were then dissociated and grown in a 6-well plate for colony formation at six hundred viable cells per well. Three replicate wells were set up for each experimental group. After 14 days, most clones contained more than 50 cells (medium was exchanged every three days). Crystal violet staining (1000 μL/well) was then performed and visualized using a microscope. Only a colony with more than 50 cells was counted.

2.9 RNA-seq

After being interfered by siLPGAT1 and siCtrl, the H1299 cell lines were extracted for RNA, and transcriptome sequencing was performed. We selected differentially expressed genes (DEGs) with |log2 fold change| $\geq$2 and a p-value < 0.05. A clustering heat map was drawn with the DEGs, and then these DEGs were detected by GO functional enrichment analysis, and the results were classified into three terms, including biological processes (BPs), cellular components (CCs) and molecular functions (MFs).

2.10 qRT-PCR

Total RNA was extracted from the H1299 cells treated with lentivirus using the TRIzol® Plus RNA Purification Kit (12183-555, Invitrogen, Carlsbad, CA, USA). RNA was reverse-transcribed by SuperScript™ III First-Strand Synthesis SuperMix (11752-050, Invitrogen, Carlsbad, CA, USA), and qPCR was performed by Power SYBR Green PCR Master Mix (4367659, Applied Biosystems, Waltham, MA, USA). The primer sequences are displayed in **Supplementary Table 1**. The CFX384 multiplex RT-PCR instrument (Bio-Rad, Berkeley, CA, USA) was employed for mRNA expression analysis. The fold-change was measured using the $2^{-\Delta\Delta Ct}$ method.

2.11 Protein Isolation and WB Analysis

A total protein extraction kit containing protease inhibitor cocktail (BC3710, Solarbio, Beijing, China) was utilized for total protein isolation. A bicinchoninic acid (BCA) quantification kit (B0010, Beyotime, Shanghai, China) was utilized for total protein quantification. After separation through 10% SDS-PAGE, the proteins were subsequently transferred onto PVDF membranes (IPVH00010, Millipore, St. Louis, MO, USA). The membranes were incubated with the primary antibodies at 4 °C overnight, followed by the secondary antibodies (Goat anti-Rabbit IgG (H+L), 31210, Thermo Pierce, Waltham, MA, USA) at RT for 1 h. The following primary antibodies were employed: anti-LPGAT1 (bs-18347r, Bioss, Woburn, MA, USA), anti-GPAM (bs-5063r, Bioss, Woburn, MA, USA), anti-LCLAT1 (bs-18190r, Bioss, Woburn, MA, USA), anti-LPCAT1(16112-1-AP, Proteintech, Wuhan, China) anti-LPCAT4 (17905-1-AP, Proteintech, Wuhan, China), anti-CRLS1 (14845-1-AP, Proteintech, Wuhan, China), and anti-α-tubulin (11224-1-AP, Proteintech, Wuhan, China). Protein bands were quantified with ImageJ software (NIH, Bethesda, MD, USA).

2.12 Nude Mouse Xenograft Studies

All the experimental protocols were conducted in accordance with the institutional ethics and safety guidelines of the same institute. Twenty-two BALB/c nude mice (female, 6 weeks old, 16–18 g) were supplied by Shanghai Lingchang Biotechnology (Shanghai, China), and were maintained at the Experimental Animal Center, and underwent a 10/14-h light-dark cycle (55 $\pm$ 5% humidity and 22 $\pm$ 1 °C). The mice were randomly assigned to four groups. LPGAT1 knockdown and control xenograft models were established by injecting 4×10^6 H1299 (or A549) cells into the right flank of mice. After 2 weeks, the tumor size was examined twice a week. Tumor length and width were determined using a caliper. Tumor volume was calculated as follows: volume (mm^3) = $\pi/6 \times$ length $\times$ width $\times$ width. Following six weeks, each mouse was euthanized by cervical dislocation, and tumor tissues were obtained. Tumor volumes were calculated as described above, and tumor weights were measured using an electronic balance.

2.13 Survival Analysis

The mRNA level of LPGAT1 was detected using the TCGA-LUAD cohort. After merging with LPGAT1 expression data, the samples with complete information on patient survival, age, gender, N stage, T stage and tumor stage were used to construct the Kaplan-Meier curve and perform univariate and multivariate Cox analyses.

2.14 Statistical Analysis

All values are shown as mean $\pm$ SD. The differences between groups were compared by Student's t-test or one-way ANOVA. p-values of <0.05 were regarded as statistically significant. All tests were performed with SPSS v18.0 (IBM, Amonk, NY, USA) and GraphPad Prism v6.0 (GraphPad Software, San Diego, CA, USA).

3. Results

3.1 LPGAT1 is Highly Expressed in LUAD and Related to Poor Prognosis

This study assessed the role of LPGAT1 in LUAD. Expression data from the Cancer Genome Atlas (TCGA-LUAD), comprising 497 LUAD tissues and 54 non-tumor tissues, were analyzed. Our results indicated that LPGAT1 was significantly increased in LUAD tissue compared to non-tumor tissue (Fig. 1A). All LUAD patients were classified into LPGAT1 high-expression and low-expression groups based on the median value of LPGAT1 expression. However, Kaplan-Meier analysis revealed that the survival rate of the LPGAT1 low-expression group was not better than that of the LPGAT1 high-expression group (Fig. 1B). In addition, after combining LPGAT1 expression data and survival data from these samples, univariate and multivariate Cox analyses were performed. The results demonstrated that LPGAT1 was an independent poor prognostic factor (**Supplementary Tables 2, 3**). 60 pairs of LUAD and neighboring normal tissues were acquired, and the following steps were performed: immunohistochemical staining, photography, interpretation, and pathological analysis. The findings were highly consistent with the above data, in which the expression of LPGAT1 was higher in LUAD tissues than in paracancer tissues (Fig. 1C). The immunohistochemical scores of the 60 clinical samples are shown

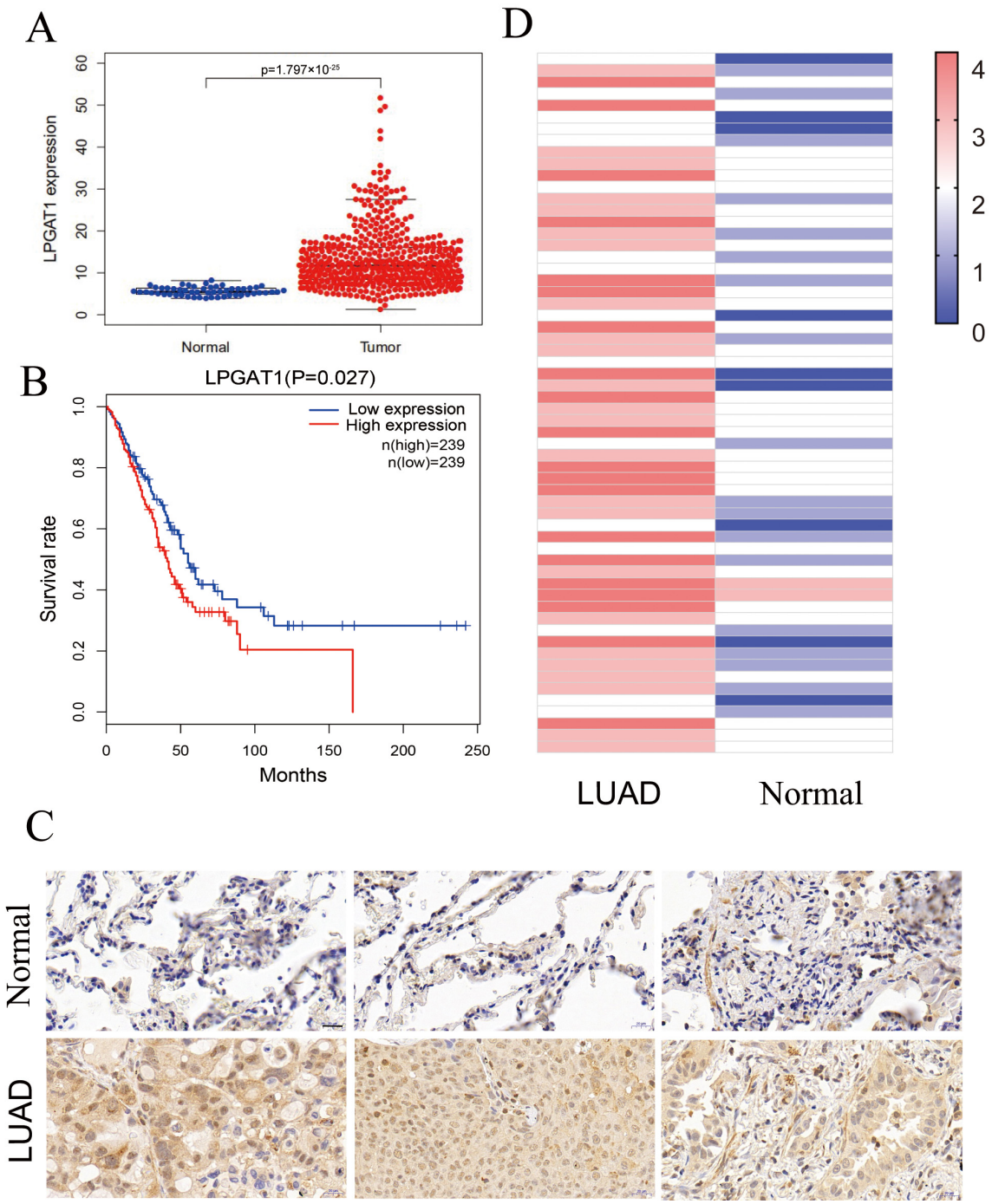

Fig. 1. LPGAT1 is highly expressed in lung adenocarcinoma tissues. (A) Statistical results of LPGAT1 expression data from TCGA-LUAD. (B) Kaplan-Meier analysis of LUAD patients' prognosis with high and low expression of LPGAT1. (C) LPGAT1 expression in tumor tissues and normal tissues via IHC staining. Scale bars: 20 μm. (D) IHC results of 60 clinical samples were scored: 0 as negative, 1 as $<$10% of positive cells, 2 as 11–50%, 3 as 51–75%, and 4 as $>$75%.

in Fig. 1D.

3.2 Upregulation of LPGAT1 Inhibits Apoptosis and Promotes Proliferation in LUAD Cell Lines

To explore the role of LPGAT1 in LUAD, a series of functional assays were performed in LUAD cells. H1299 and A549 cells with the highest LPGAT1 expression were selected for the subsequent analyses (Fig. 2A and **Supplementary Fig. 1A,B**). These LUAD cell lines were transfected with siLPGAT1 and siCtrl, and qPCR assays were then conducted to detect the endogenous LPGAT1 expression. It was observed that the expression of LPGAT1 was downregulated by 95% in H1299 cells (Fig. 2B) and 88% in A549 cells (**Supplementary Fig. 1C**). Next,

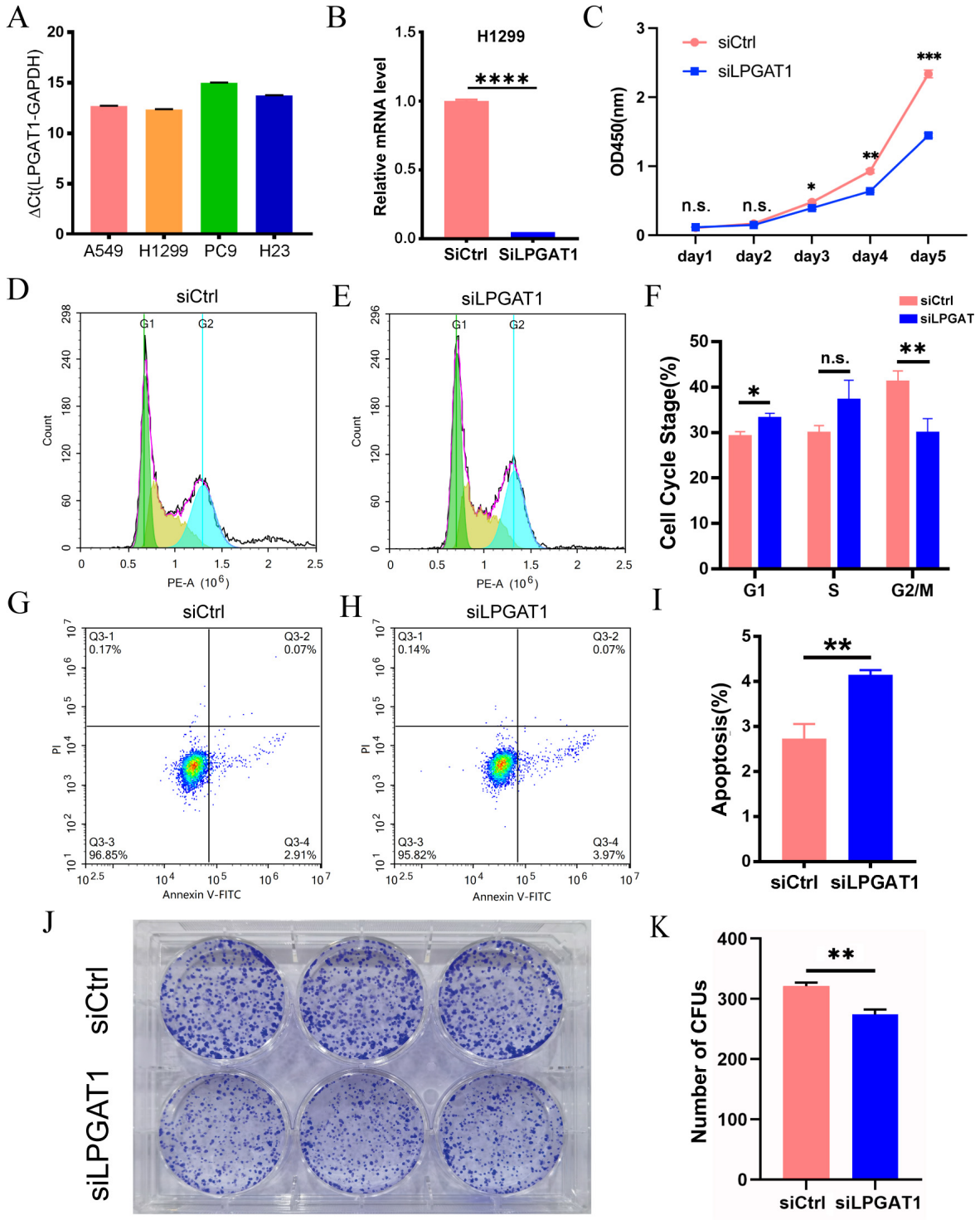

Fig. 2. Knockdown of LPGAT1 inhibits cell proliferation and promotes cell apoptosis in H1299 cell lines. (A,B) The expression levels of LPGAT1 in four NSCLC cell lines (A549, H1299, PC9, and H23), and the knockdown efficiency of siLPGAT1 in H1299, were detected by qRT-PCR. Unpaired two-tailed *t*-test; $^{****}p < 0.0001$. (C) Cell Counting Kit-8 assay was used to detect H1299 cell proliferation, n = 3. Two-way ANOVA. $^{*}p = 0.0262$ (day 3), $^{**}p = 0.0030$ (day 4), $^{***}p = 0.0006$ (day 5). (D,E) The cell cycles in the control (D) and LPGAT1-knockdown groups (E) were detected by flow cytometry, n = 3. (F) Statistical results of the cell cycle assay. Unpaired two-tailed *t*-test; $^{*}p = 0.0115$ (G1 phase), $^{ns}p = 0.0552$ (S phase), $^{**}p = 0.0087$ (G2/M phase). (G,H) Cell apoptosis in the control (G) and LPGAT1-knockdown groups (H) was detected by flow cytometry, n = 3. (I) Statistical results of cell apoptosis assay. Unpaired two-tailed *t*-test; $^{**}p = 0.0019$. (J) Colony formation assay, n = 3. (K) Statistical results of the colony formation assay. Unpaired two-tailed *t*-test; $^{**}p = 0.0015$.

CCK-8, FC and CFA were conducted on the stable transfected LUAD cells to assess cell proliferation and apoptosis. The findings of CCK-8 assays demonstrated that the proliferation of H1299 cell line (Fig. 2C) and A549 cell line (**Supplementary Fig. 1D,E**) was attenuated by LPGAT1 knockdown. FC analysis revealed that, compared to the control group, the LPGAT1-knockdown group inhibited the cell cycle progression, G2/M cells were decreased, and G1 cells were increased in H1299 cell lines (Fig. 2D–F and **Supplementary Fig. 1F**), while only G1 cells were increased in A549 cell lines (**Supplementary Fig. 1G,H**). The green-, yellow-, and blue-emitting populations in the latter corresponded to G1, G1/S and S/G2-M cells, respectively. In addition, the data of FC indicated that the apoptotic rate of LUAD cells was dramatically elevated after LPGAT1 knockdown (Fig. 2G–I, **Supplementary Fig. 1I,J** and **Supplementary Fig. 2A**). Furthermore, the findings of CFA showed that the number of colonies was decreased in H1299 cells with LPGAT1 knockdown (Fig. 2J,K).

3.3 LPGAT1 Knockdown Suppresses LUAD Progression in Vivo

A BALB/cnu/nu nude mouse xenograft model was constructed by subcutaneously injecting H1299 cells to investigate whether LPGAT1 knockdown can suppress LUAD progression *in vivo*. H1299 cells were transfected with lentiviruses (shCtrl and shLPGAT1) for 48 h (Fig. 3A). The infection efficiency of the lentivirus was 93.6% and 94.1%, respectively (**Supplementary Fig. 2B**). Eight mice were subcutaneously injected with shCtrl-infected H1299 cells (4×10^6 each) into the right flanks, while the other eight mice were injected with shLPGAT1-infected H1299 cells (Fig. 3B). Consistent with the *in vitro* results, the LPGAT1 knockdown group had a more significant inhibitory effect on tumor volume growth in a time-dependent fashion (Fig. 3C). After 4 weeks, tumors were peeled from the nude mouse subcutis. Then, the tumors were weighed (Fig. 3D) and their length and width were measured to calculate the tumor volumes (Fig. 3E–G). The results of the experiments performed with A549 cells were similar to those of the H1299 cells (**Supplementary Fig. 2C,D**). The tumors in the shLPGAT1 group were smaller in size and lower in weight compared with those in the control group.

3.4 Upregulation of LPGAT1 Promotes LUAD Progression via Phosphatidylglycerol Metabolic Process

After the knockdown of LPGAT1, H1299 cells were collected for RNA-Seq. 106 DEGs are shown in the heatmap (Fig. 4A). These genes were detected by GO enrichment analysis; the top 10 results in BPs, CCs, and MFs are shown in Fig. 4B and **Supplementary Table 4**. We found the most prominent regulation involved the phosphatidylglycerol metabolic pathway, phosphatidylglycerol acyl-chain remodeling, the phosphatidic acid biosynthetic process, the phosphatidic acid metabolic processes, and the phospholipid biosynthetic process in BPs. There were five common genes in the five most prominent pathways, namely LPCAT4, LPCAT1, Lyso-CL acyltransferase 1 (LCLAT1), Glycerol-3-phosphate acyltransferase mitochondrial (GPAM), and cardiolipin synthase 1 (CRLS1). In order to verify the effect of target gene LPGAT1 knockdown on these pathways, we performed qRT-PCR and WB analyses. Based on the qRT-PCR data, these genes were upregulated in H1299 cells with LPGAT1 knockdown compared to the control group (Fig. 5A–E). However, WB analysis demonstrated that the levels of CRLS1, GPAM and LPLAT1 proteins had an upward trend in H1299 cells with LPGAT1 knockdown, but no statistical significance was observed. Similarly, there was no marked difference in the expression of LPCAT1 and LPCAT4 between the two groups (Fig. 5F,G).

4. Discussion

LC is a leading cause of cancer-related mortality worldwide, with around 1.76 million deaths and 2 million new cases annually [16]. Existing studies [17,18] have shown that the development and progression of LC is closely associated with lipid metabolism.

LPGAT1 regulates triacylglycerol biosynthesis and is essential for maintaining phospholipid homeostasis and modulating the structural integrity of the mitochondrial membrane [11]. It has been reported that LPGAT1 is differentially expressed in normal and tumor tissues [14]. It is a target gene for upregulated expression of miRNAs in LUAD and may be involved in lipid metabolic processes. A previous study has proposed that LPGAT1 can remodel phosphatidylglycerol, an intermediate of the cardiolipin (CL) pathway. LPGAT1 is of central importance for the regulation of lipid metabolism [19,20].

In this study, we confirmed that the expression of LPGAT1 in LUAD tissues was higher than that in adjacent tissues by IHC in 60 pairs of clinical samples. This study is the first to demonstrate that LPGAT1 knockdown could inhibit the progression of NSCLC in both human cell lines and mouse models. In the cell lines, after knockdown of LPGAT1, cell proliferation was inhibited as shown by the CCK-8 assay, apoptosis was increased, and the cell cycle was arrested as shown by FC. In *in vivo* experiments in mice, tumor growth was also inhibited in the knockdown group compared to the controls. Thus, in addition to previous reports [19,20], we further clarified the role of LPGAT1 in LUAD progression, and hypothesized that the inhibition of tumor growth after LPGAT1 knockdown was related to lipid metabolism. We performed transcriptome sequencing to further explore this concept.

After the transcriptome sequencing of H1299 cell lines in the LPGAT1 knockdown and control groups, GO enrichment analysis was performed to screen the up-regulated pathways and pathway-related genes (CRLS1, GPAM, LCLAT1, LPCAT1, LPCAT4). The functions of these

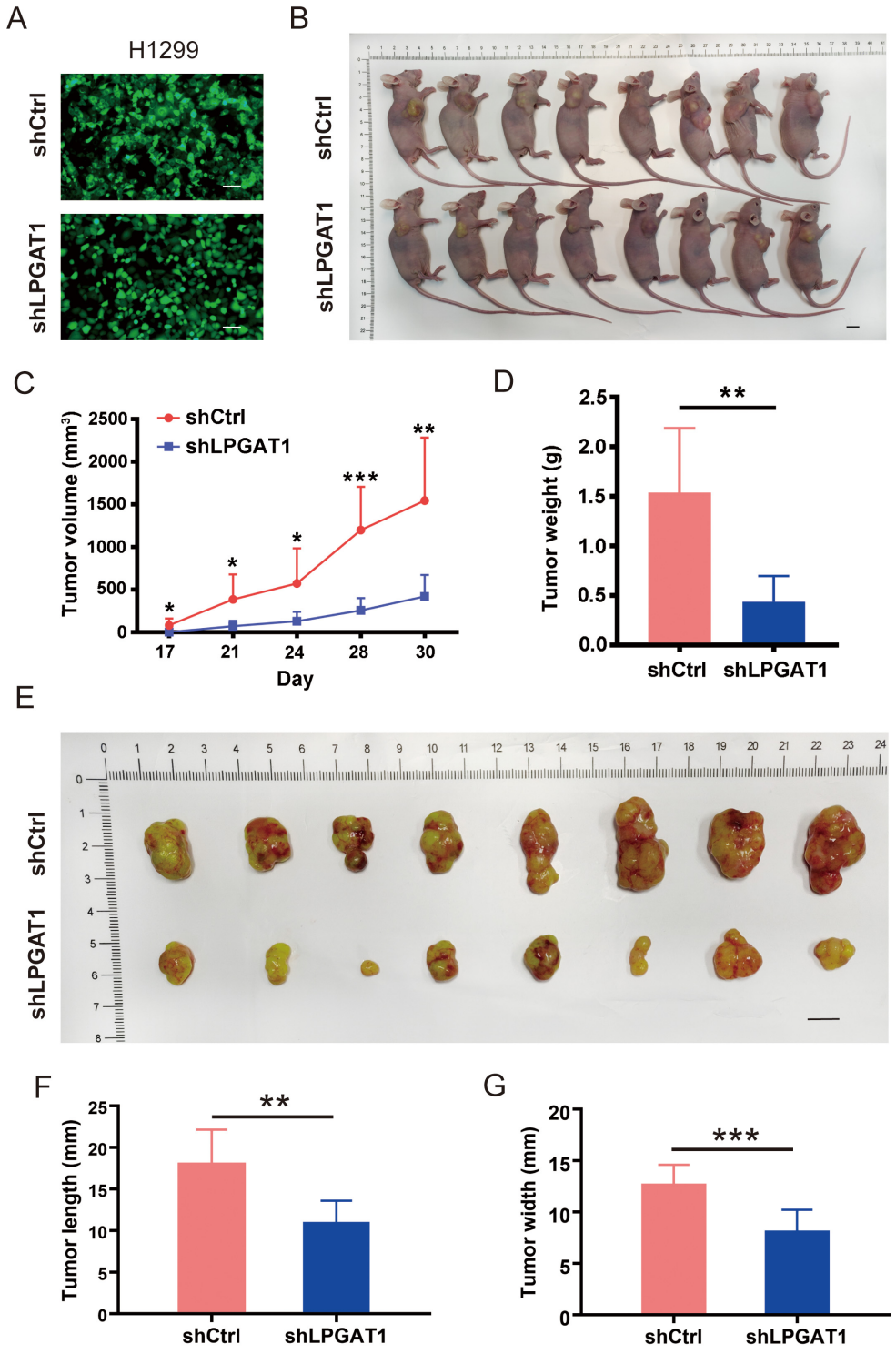

Fig. 3. Knockdown of LPGAT1 inhibits tumor growth in tumor-bearing mice. (A) Infection efficiency of lentiviruses (shCtrl and shLPGAT1) in H1299 cells. Scale bars: 25 μm. (B) *In vivo* imaging of tumor-bearing mice in the control and LPGAT1-knockdown groups, n = 8. Scale bars: 1 cm. (C, D) Measurement of the volume and weight of tumors. C, measure the volume of tumors twice a week since 17 days after injection, volume (mm^3) = $\pi/6 \times$ length $\times$ width $\times$ width; $^{*}p = 0.0124$ (at day 17), $^{*}p = 0.0106$ (at day 21), $^{*}p = 0.0110$ (at day 24), $^{***}p = 0.0002$ (at day 28), $^{**}p = 0.0011$ (at day 30); (D) tumors were peeled and then weighed after 4 weeks, Welch *t*-test, $^{**}p = 0.0015$ (tumor weight). (E) Tumor size was measured in the control and LPGAT1-knockdown groups. Scale bars: 1 cm. (F, G) Statistical analysis of the differences in length and width between the two groups of tumors. $^{**}p = 0.0017$ (tumor length), $^{***}p = 0.0006$ (tumor width).

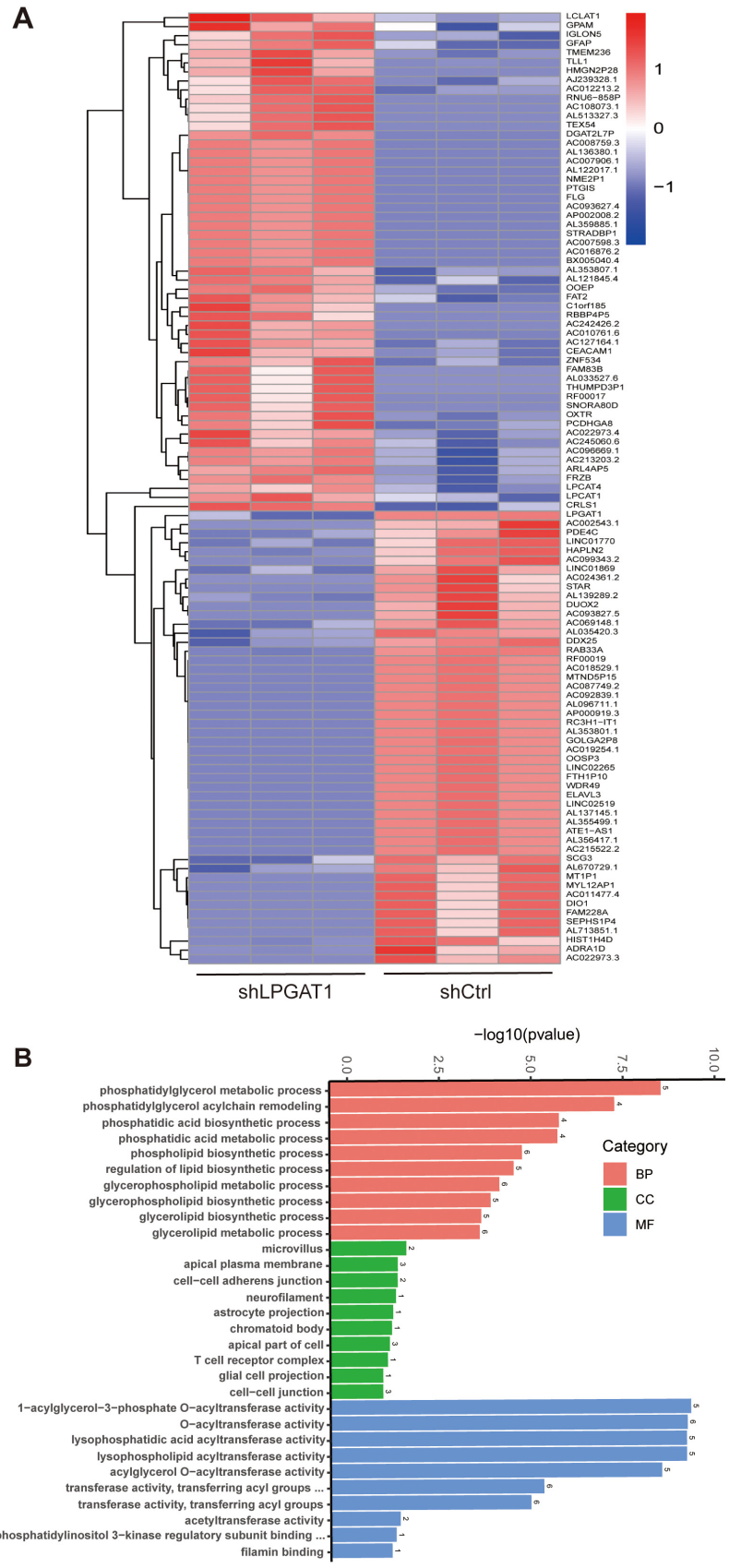

Fig. 4. Heatmap of DEGs and GO functional enrichment analysis after LPGAT1 knockdown in H1299 cell lines. (A) Heatmap of differentially expressed genes between the control group (on the right) and the shLPGAT1 group (on the left). (B) Top 30 GO terms, including biological processes (BPs), cellular components (CCs) and molecular functions (MFs).

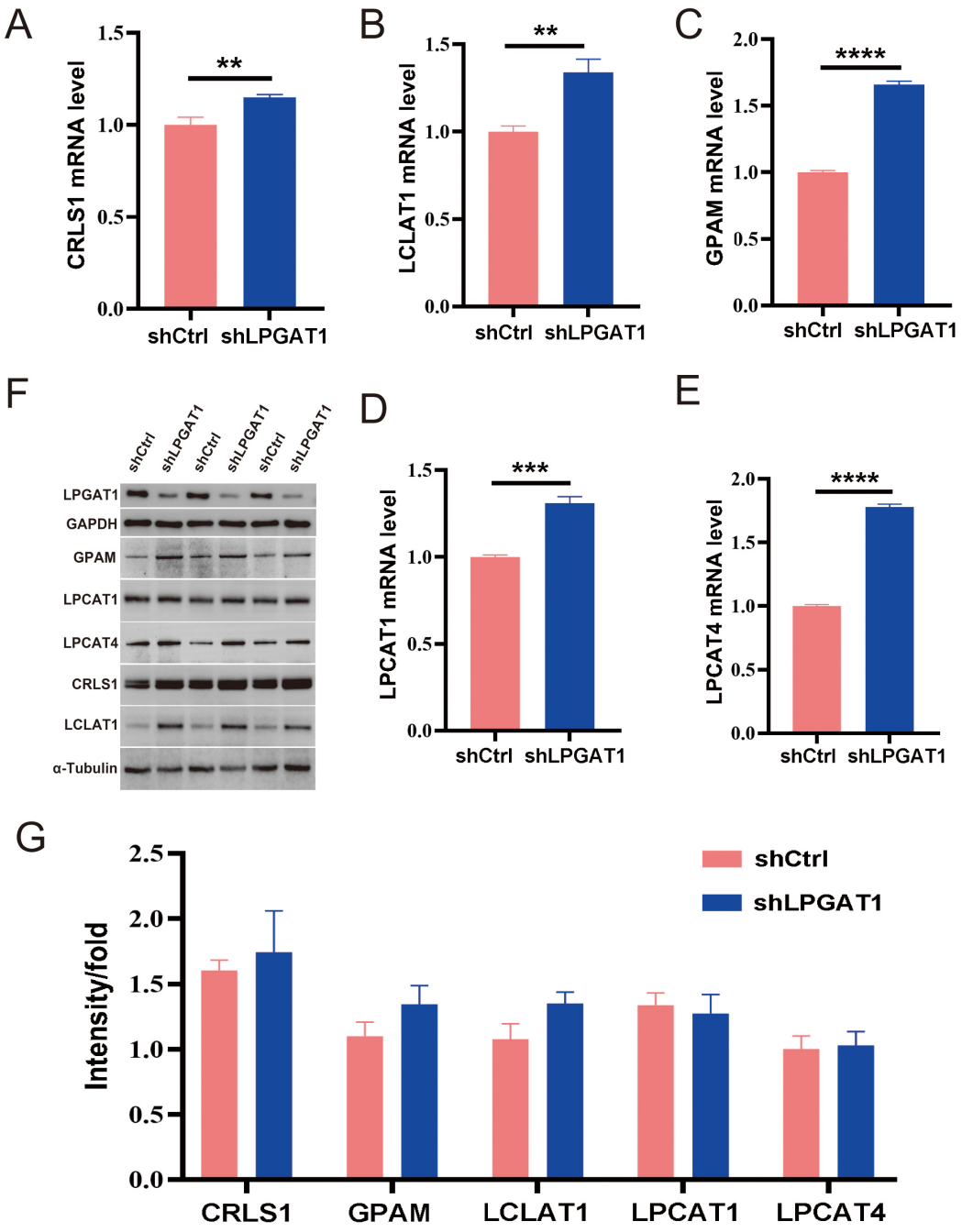

Fig. 5. Expression of the related proteins after LPGAT1 knockdown in H1299 cell lines. (A–E) The mRNA levels of CRLS1, LCLAT1, GPAM, LPCAT1 and LPCAT4 in the shCtrl and shLPGAT1 groups. Unpaired two-tailed *t*-test; $^{**}p = 0.0052$ (CRLS1), $^{**}p = 0.0021$ (LCLAT1), $^{****}p < 0.0001$ (GPAM), $^{***}p = 0.0001$ (LPCAT1),$^{****}p < 0.0001$ (LPCAT4). (F) The protein levels of CRLS1, LCLAT1, GPAM, LPCAT1 and LPCAT4 in the shCtrl and shLPGAT1 groups. (G) Statistical results of protein expression intensity.

genes have also been reported. LPCAT catalyzes the conversion of Lys phosphatidylcholine to phosphatidylcholine, thereby remodeling the biosynthesis pathway [21]. GPAM has been reported to play a vital role in lipid biosynthesis; especially phospholipid synthesis [22]. Human CRLS1 is critical for CL synthesis and phosphatidylglycerol remodeling [23,24]. CLs are specific phospholipids of the mitochondria [25–27]. LCLAT1 localizes in the mitochondria-associated membrane [28], and its overexpression elevates the levels of polyunsaturated fatty acids containing CL [28–30], all of which are related to lipid metabolism. Therefore, we speculate that the downregulation of LPGAT1 affects lipid metabolism and the expression of these genes. Subsequently, we verified the genes by qPCR, and the knockdown group showed significant up-regulation compared to the control group. However, WB results showed no significant difference in protein-level expression of these genes between the two groups. Thus, further exploration of the in-

teraction between LPGAT1 and these pathway related genes is still needed, and will be examined in future studies.

5. Conclusions

In conclusion, our study revealed that LPGAT1 plays a critical role in the tumorigenesis of NSCLC. These experimental results demonstrated that knockdown of LPGAT1 inhibited tumor growth, which was characterized by inhibited cell proliferation and the induction of cell apoptosis. Nevertheless, the mechanism by which LPGAT1 promotes LUAD needs to be further investigated. In conclusion, LPGAT1 may serve as a new therapeutic target for treatment of LUAD.

Availability of Data and Materials

The original contributions presented in the study are included inthe article/**Supplementary Material**. Further inquiries can bedirected to the corresponding authors.

Author Contributions

HG, XW, CM and NW conceived the experiments. XW and NW designed the experiments. HG, CM, XL, YH, PC, XZ and LZ conducted the experiment. TH and WW performed bioinformatics analyses. All the authors analyzed and discussed the results. HG, XW, NW guided the work. HG, CM wrote the first draft. NW, XW revised the first draft. All authors contributed to editorial changes in the manuscript. All authors read and approved the final manuscript. All authors have participated sufficiently in the work to take public responsibility for appropriate portions of the content and agreed to be accountable for all aspects of the work in ensuring that questions related to its accuracy or integrity.

Ethics Approval and Consent to Participate

The studies involving human participants were reviewed and approved by the Ethics Review Committee of the First Affiliated Hospital of Bengbu Medical College (approval no. 2021KY092). The patients/participants provided their written informed consent to participate in this study. The animal study was reviewed and approved by the Ethics Review Committee of the First Affiliated Hospital of Bengbu Medical College (approval no. 2021-268).

Acknowledgment

Thanks to the First Affiliated Hospital of Bengbu Medical College for his permission to publish this article. We would also like to extend special thanks to the technical staff of Anhui Clinical and Preclinical Key Laboratory of Respiratory Disease for their excellent laboratory assistance. Moreover, we thank all the clinicians of Thoracic Surgery Department who participated in the patient's management.

Funding

This work was supported by the Key Program of Natural Science Research of Higher Education of Anhui Province (grant KJ2020A0575); National Natural Science Foundation of China (82072585); Anhui Provincial Major Science and Technology Project (202003a07020024).

Conflict of Interest

The authors declare no conflict of interest.

Supplementary Material

Supplementary material associated with this article can be found, in the online version, at https://doi.org/10.31083/j.fbl2805089.

References

[1] Siegel RL, Miller KD, Jemal A. Cancer statistics, 2019. CA: A Cancer Journal for Clinicians. 2019; 69: 7–34.

[2] Siegel RL, Miller KD, Fuchs HE, Jemal A. Cancer statistics, 2022. CA: A Cancer Journal for Clinicians. 2022; 72: 7–33.

[3] Simó M, Vaquero L, Ripollés P, Gurtubay-Antolin A, Jové J, Navarro A, *et al*. Longitudinal Brain Changes Associated with Prophylactic Cranial Irradiation in Lung Cancer. Journal of Thoracic Oncology: Official Publication of the International Association for the Study of Lung Cancer. 2016; 11: 475–486.

[4] Shahabi S, Kumaran V, Castillo J, Cong Z, Nandagopal G, Mullen DJ, *et al*. LINC00261 Is an Epigenetically Regulated Tumor Suppressor Essential for Activation of the DNA Damage Response. Cancer Research. 2019; 79: 3050–3062.

[5] Kim HS, Mitsudomi T, Soo RA, Cho BC. Personalized therapy on the horizon for squamous cell carcinoma of the lung. Lung Cancer (Amsterdam, Netherlands). 2013; 80: 249–255.

[6] Xue M, Tao W, Yu S, Yan Z, Peng Q, Jiang F, *et al*. lncRNA ZFPM2-AS1 promotes proliferation via miR-18b-5p/VMA21 axis in lung adenocarcinoma. Journal of Cellular Biochemistry. 2020; 121: 313–321.

[7] Li S, Choi YL, Gong Z, Liu X, Lira M, Kan Z, *et al*. Comprehensive Characterization of Oncogenic Drivers in Asian Lung Adenocarcinoma. Journal of Thoracic Oncology: Official Publication of the International Association for the Study of Lung Cancer. 2016; 11: 2129–2140.

[8] Thai AA, Solomon BJ, Sequist LV, Gainor JF, Heist RS. Lung cancer. Lancet (London, England). 2021; 398: 535–554.

[9] O'Farrell H, Harbourne B, Kurlawala Z, Inoue Y, Nagelberg AL, Martinez VD, *et al*. Integrative Genomic Analyses Identifies GGA2 as a Cooperative Driver of EGFR-Mediated Lung Tumorigenesis. Journal of Thoracic Oncology: Official Publication of the International Association for the Study of Lung Cancer. 2019; 14: 656–671.

[10] Yang Y, Cao J, Shi Y. Identification and Characterization of a Gene Encoding Human LPGAT1, an Endoplasmic Reticulum-associated Lysophosphatidylglycerol Acyltransferase. Journal of Biological Chemistry. 2004; 279: 55866–55874.

[11] Wei Z, Zhao J, Niebler J, Hao JJ, Merrick BA, Xia M. Quantitative Proteomic Profiling of Mitochondrial Toxicants in a Human Cardiomyocyte Cell Line. Frontiers in Genetics. 2020; 11: 719.

[12] Traurig MT, Orczewska JI, Ortiz DJ, Bian L, Marinelarena AM, Kobes S, *et al*. Evidence for a role of LPGAT1 in influencing BMI and percent body fat in Native Americans. Obesity (Silver Spring, Md.). 2013; 21: 193–202.

[13] Hou J, Aerts J, den Hamer B, van Ijcken W, den Bakker M, Riegman P, *et al*. Gene expression-based classification of non-small

cell lung carcinomas and survival prediction. PLoS ONE. 2010; 5: e10312.

[14] Geng Y, Deng L, Su D, Xiao J, Ge D, Bao Y, *et al*. Identification of crucial microRNAs and genes in hypoxia-induced human lung adenocarcinoma cells. OncoTargets and Therapy. 2016; 9: 4605–4616.

[15] Yu X, Zhang X, Zhang Y. Identification of a 5-Gene Metabolic Signature for Predicting Prognosis Based on an Integrated Analysis of Tumor Microenvironment in Lung Adenocarcinoma. Journal of Oncology. 2020; 2020: 5310793.

[16] Singh D, Vignat J, Lorenzoni V, Eslahi M, Ginsburg O, Lauby-Secretan B, *et al*. Global estimates of incidence and mortality of cervical cancer in 2020: a baseline analysis of the WHO Global Cervical Cancer Elimination Initiative. The Lancet. Global Health. 2023; 11: e197–e206.

[17] Merino Salvador M, Gómez de Cedrón M, Moreno Rubio J, Falagán Martínez S, Sánchez Martínez R, Casado E, *et al*. Lipid metabolism and lung cancer. Critical Reviews in Oncology/hematology. 2017; 112: 31–40.

[18] Wang G, Qiu M, Xing X, Zhou J, Yao H, Li M, *et al*. Lung cancer scRNA-seq and lipidomics reveal aberrant lipid metabolism for early-stage diagnosis. Science Translational Medicine. 2022; 14: eabk2756.

[19] Xu Y, Miller PC, Phoon CKL, Ren M, Nargis T, Rajan S, *et al*. LPGAT1 controls the stearate/palmitate ratio of phosphatidylethanolamine and phosphatidylcholine in sn-1 specific remodeling. The Journal of Biological Chemistry. 2022; 298: 101685.

[20] Zhang X, Zhang J, Sun H, Liu X, Zheng Y, Xu D, *et al*. Defective Phosphatidylglycerol Remodeling Causes Hepatopathy, Linking Mitochondrial Dysfunction to Hepatosteatosis. Cellular and Molecular Gastroenterology and Hepatology. 2019; 7: 763–781.

[21] Du Y, Wang Q, Zhang X, Wang X, Qin C, Sheng Z, *et al*. Lysophosphatidylcholine acyltransferase 1 upregulation and concomitant phospholipid alterations in clear cell renal cell carcinoma. Journal of Experimental & Clinical Cancer Research: CR. 2017; 36: 66.

[22] Brockmöller SF, Bucher E, Müller BM, Budczies J, Hilvo M, Griffin JL, *et al*. Integration of metabolomics and expression of glycerol-3-phosphate acyltransferase (GPAM) in breast cancer-link to patient survival, hormone receptor status, and metabolic profiling. Journal of Proteome Research. 2012; 11: 850–860.

[23] Feng HM, Zhao Y, Zhang JP, Zhang JH, Jiang P, Li B, *et al*. Expression and potential mechanism of metabolism-related genes and CRLS1 in non-small cell lung cancer. Oncology Letters. 2018; 15: 2661–2668.

[24] Luévano-Martínez LA, Duncan AL. Origin and diversification of the cardiolipin biosynthetic pathway in the Eukarya domain. Biochemical Society Transactions. 2020; 48: 1035–1046.

[25] Horvath SE, Daum G. Lipids of mitochondria. Progress in Lipid Research. 2013; 52: 590–614.

[26] Ahmadpour ST, Mahéo K, Servais S, Brisson L, Dumas JF. Cardiolipin, the Mitochondrial Signature Lipid: Implication in Cancer. International Journal of Molecular Sciences. 2020; 21: 8031.

[27] Paradies G, Paradies V, Ruggiero FM, Petrosillo G. Role of Cardiolipin in Mitochondrial Function and Dynamics in Health and Disease: Molecular and Pharmacological Aspects. Cells. 2019; 8: 728.

[28] Li J, Romestaing C, Han X, Li Y, Hao X, Wu Y, *et al*. Cardiolipin remodeling by ALCAT1 links oxidative stress and mitochondrial dysfunction to obesity. Cell Metabolism. 2010; 12: 154–165.

[29] Li Z, Ding T, Pan X, Li Y, Li R, Sanders PE, *et al*. Lysophosphatidylcholine acyltransferase 3 knockdown-mediated liver lysophosphatidylcholine accumulation promotes very low density lipoprotein production by enhancing microsomal triglyceride transfer protein expression. The Journal of Biological Chemistry. 2012; 287: 20122–20131.

[30] Liu X, Ye B, Miller S, Yuan H, Zhang H, Tian L, *et al*. Ablation of ALCAT1 mitigates hypertrophic cardiomyopathy through effects on oxidative stress and mitophagy. Molecular and Cellular Biology. 2012; 32: 4493–4504.